Science & Nanotechnology
DOI: 10.64214/jmsn.01.03004 Communication

Epitaxial-strain control of quantum conductance corrections and weak antilocalization in $SrIrO_3$ thin films*

G. D. Ulev,[1,2] G. A. Ovsyannikov,[1] A. V. Mashirov,[1] I. E. Moskal[1]

[1] *Kotelnikov Institute of Radio Engineering and Electronics, Russian Academy of Sciences, Moscow, Russia*
[2] *Moscow Institute of Physics and Technology, Dolgoprudny, Russia*

submitted 27 July 2026, accepted 30 August 2026, published 08 September 2026

We study the low-temperature quantum conductance corrections in epitaxial $SrIrO_3$ thin films grown on substrates that impose biaxial strain of different sign and magnitude. The most instructive pair is the films on $Pb(Mg_{1/3}Nb_{2/3})O_3$–$PbTiO_3$ (PMN-PT) and $SrTiO_3$, which carry strain of opposite sign and nearly equal magnitude – tensile $\varepsilon = +1.5\%$ and compressive $\varepsilon = -1.4\%$ – while $NdGaO_3$ and $(LaAlO_3)_{0.3}(Sr_2TaAlO_6)_{0.7}$ (LSAT) provide progressively stronger compression. In all films the resistivity rises logarithmically on cooling, the signature of two-dimensional quantum corrections, and the magnetoconductance is well described by the two-dimensional Maekawa-Fukuyama model with a classical quadratic orbital background. The sign of the strain governs the character of the corrections: the tensile PMN-PT film sustains weak antilocalization, seen as a zero-field conductance peak, whereas the compressive films cross over to weak localization, where the magnetoconductance is parabolic and shows no peak – the Maekawa–Fukuyama model describes both regimes equally well. The extracted phase-coherence length follows the temperature dependence expected for two-dimensional electron-electron (Coulomb) scattering, confirming the two-dimensional nature of the corrections despite the finite film thickness. The tensile and weakly compressed films display an intrinsic, hysteresis-free anomalous Hall effect of Berry-curvature origin, which is suppressed under the strongest compression. The sign and magnitude of the substrate-imposed strain thus govern the quantum conductance corrections in $SrIrO_3$ thin films.

Introduction

Strontium iridate $SrIrO_3$ is a nonsymmorphic Dirac semimetal with strong spin-orbit coupling (SOC, $\simeq 0.5$ eV), in which the linear bands near the Dirac points are protected by the glide symmetry of the Pbnm space group.[1,2] Epitaxial strain imposed by the substrate breaks this symmetry and modifies the IrO_6 octahedra, which changes both the band structure and the effective SOC seen in transport.[2,3] At low temperatures this strong SOC gives rise to quantum conductance corrections – weak antilocalization (WAL) – whose analysis yields the characteristic dephasing and spin-orbit lengths.[3,4] How the sign of the substrate-imposed strain controls these corrections has remained unexplored; in particular, $Pb(Mg_{1/3}Nb_{2/3})O_3$-$PbTiO_3$ (PMN-PT) substrates had not been used for $SrIrO_3$ growth before. Here we compare $SrIrO_3$/PMN-PT (tensile, $\varepsilon = +1.5\%$) and $SrIrO_3/SrTiO_3$ (compressive, $\varepsilon = -1.4\%$), 35 nm thick, over 2–50 K. Films deposited on $NdGaO_3$ and $(LaAlO_3)_{0.3}(Sr_2TaAlO_6)_{0.7}$ (LSAT) were also studied with compression $\varepsilon = -2.5\%$ and $\varepsilon = -2.3\%$.

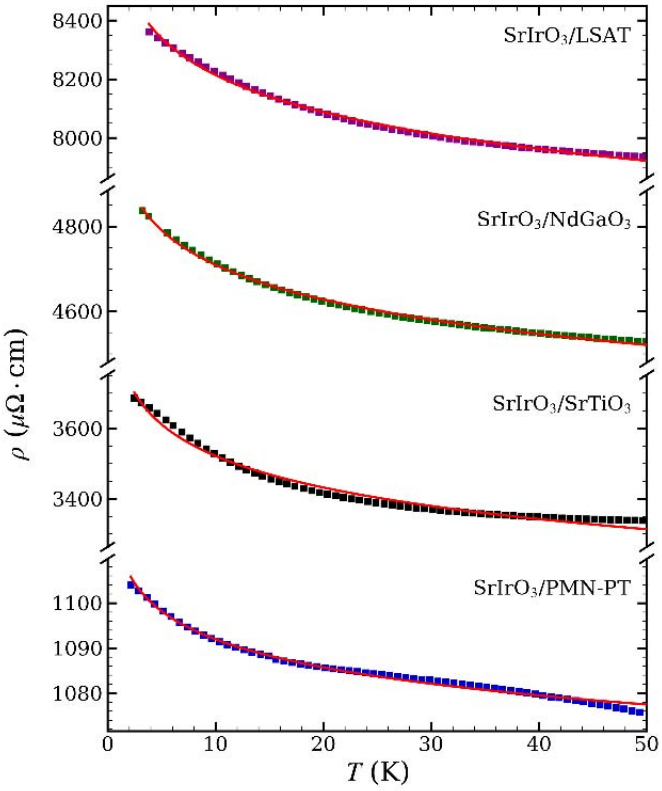


Figure 1. Resistivity ρ vs. temperature for $SrIrO_3$/LSAT, $SrIrO_3/NdGaO_3$, $SrIrO_3/SrTiO_3$ and $SrIrO_3$/PMN-PT (top to bottom) over $2-50$ K. Red lines: logarithmic fits according to Eq. (1).

Methods

The films were deposited by radio frequency magnetron sputtering; X-ray diffraction confirmed epitaxial growth with out-of-plane parameters $c = 3.94$ Å(PMN-PT) and $c = 4.03$Å($SrTiO_3$) relative to the bulk pseudocubic $a_0 = 3.96$ Å, giving $\varepsilon = +1.5\%$ and -1.4%, respectively.[5] Magnetotransport was measured on Hall bar bridges in fields

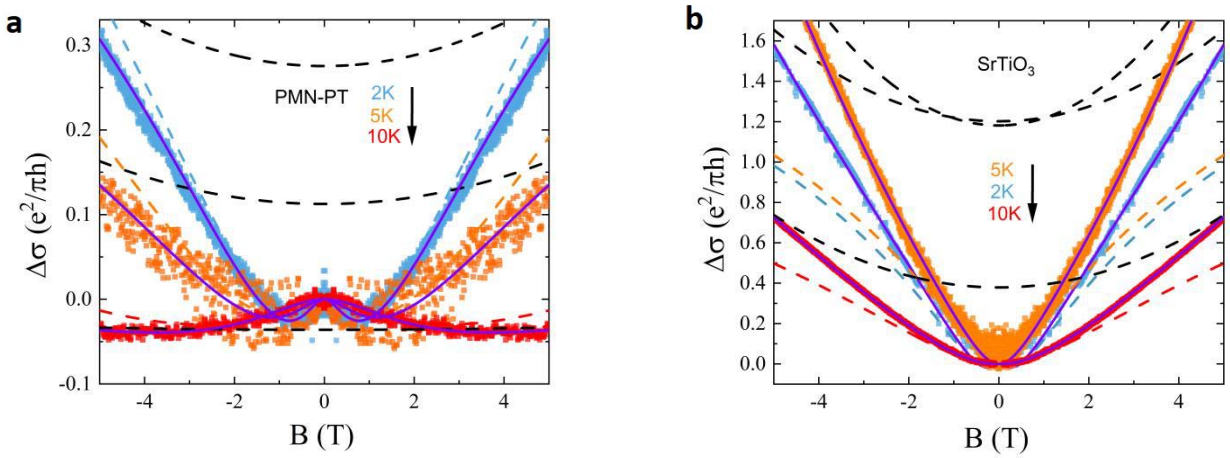


Figure 2. Magnetoconductance $\Delta\sigma(B)$ at 2–10 K fitted by the Maekawa–Fukuyama model with a classical B^2 background. **a** – $SrIrO_3$/PMN-PT; **b** – $SrIrO_3$/$SrTiO_3$. Black dashed lines: $C \cdot B^2$ term; colored dashed lines: Maekawa–Fukuyama term; solid purple lines: total fit.

up to 10 T in the low temperature range 2-10 K.

Results and discussion

For all four films residual resistivity $\rho(T)$ increases on cooling and follows the logarithmic law

$$\rho(T) = \rho_0 - A \cdot \ln\left(\frac{T}{T_0}\right), \tag{1}$$

the fingerprint of two-dimensional quantum corrections (see figure 1); A and ρ_0 are fitting parameters, $T_0 = 1\,\mathrm{K}$. The residual resistivity increases strongly with the degree of compression, being lowest for the tensile $SrIrO_3$/PMN-PT film and highest for the most strongly compressed $SrIrO_3$/LSAT film. The amplitude is much larger for $SrIrO_3$/$SrTiO_3$ ($A = 122\,\mu\Omega\cdot$cm) than for $SrIrO_3$/PMN-PT ($A = 8.7\,\mu\Omega\cdot$cm): under compressive strain the weak-localization and electron–electron contributions add, whereas under tensile strain the WAL correction partially compensates the electron-electron term.[6]

The magnetoconductance $\Delta\sigma(B) = \sigma(B) - \sigma(0)$ was fitted (figure 2) by the two-dimensional Maekawa-Fukuyama model plus a classical quadratic term[7]

$$\Delta\sigma(B) = \frac{e^2}{2\pi^2\hbar}\left[-\Psi\left(\frac{1}{2}+\frac{B_e}{B}\right) + \right.$$
$$+\frac{3}{2}\Psi\left(\frac{1}{2}+\frac{B_\varphi + B_{\mathrm{SO}}}{B}\right) - \frac{1}{2}\Psi\left(\frac{1}{2}+\frac{B_\varphi}{B}\right)$$
$$\left. - \ln\left(\frac{B_\varphi + B_{\mathrm{SO}}}{B_e}\right) - \frac{1}{2}\ln\left(\frac{B_\varphi + B_{\mathrm{SO}}}{B_\varphi}\right)\right] +$$
$$+ C \cdot B^2 \tag{2}$$

with $B_\varphi = \hbar/(4eL_\varphi^2)$, $B_{\mathrm{SO}} = \hbar/(4eL_{\mathrm{SO}}^2)$, and $B_e = \hbar/(4eL_e^2)$ the dephasing, spin-orbit and elastic characteristic fields, and Ψ the digamma function.[7]

The extracted lengths are collected in table 1. In $SrIrO_3$/PMN-PT the condition $B_{\mathrm{SO}} > B_\varphi/2$ holds at all temperatures and the WAL peak is well resolved ($L_{\mathrm{SO}} \simeq L_\varphi \simeq 13 - 26\,\mathrm{nm}$). In $SrIrO_3$/$SrTiO_3$ the classical $C \cdot B^2$ term is an order of magnitude larger and masks the peak; for $T \geq 5\,\mathrm{K}$ the film crosses over to weak localization ($B_{\mathrm{SO}}/B_\varphi < 0.5$). The elastic length $L_e \simeq 1\,\mathrm{nm} \ll L_\varphi$ in both films, and $L_\varphi \propto T^{-p/2}$ with $p \simeq 1$ confirms two-dimensional Coulomb dephasing despite the 35 nm thickness.[8]

This difference is mirrored in the magnetoresistance: $SrIrO_3$/$SrTiO_3$ shows a V-shaped negative magnetoresistance down to -3.3% at 10 T (quantum correction plus orbital B^2 background), whereas $SrIrO_3$/PMN-PT shows a much smaller signal ($\simeq -0.1\%$) with a distinct zero-field WAL peak. In addition, both paramagnetic films display a hysteresis-free, S-shaped anomalous Hall effect of intrinsic Berry-curvature origin, associated with the $J_{\mathrm{eff}} = 1/2$ states and strong SOC.[9,10] The films grown on $NdGaO_3$ and LSAT show no anomalous Hall effect at any temperature. This suggests that beyond a compressive strain of about -2.3% the epitaxial distortion widens the gap at the Dirac (nodal-line) crossings and shifts the Berry-curvature hot spots away from the Fermi level, so that the intrinsic, field-induced anomalous Hall response of the $J_{\mathrm{eff}} = 1/2$ states can no longer develop.

Conclusion

The sign and the mismatch value of the substrate-imposed epitaxial strain control the low-temperature quantum conductance corrections of $SrIrO_3$ thin films. Tensile strain (PMN-PT) sustains weak antilocalization up to 10 K, whereas compressive strain ($SrTiO_3$) drives a crossover to weak localization with a large orbital B^2 magnetoresistance. The Maekawa–Fukuyama analysis gives L_φ, $L_{\mathrm{SO}} = 13 - 42$ nm, $L_e \simeq 1\,\mathrm{nm}$ and $p \simeq 1$, confirming two-dimensional Coulomb dephasing. The more strongly compressed $NdGaO_3$ and LSAT films follow the same trend, extending the strain–correction correlation into a continuous series.

Film	T, K	L_φ, nm	L_{SO}, nm	L_e, nm
$SrIrO_3$/PMN-PT ($\varepsilon = +1.5\%$)	2.4	26.2	22.0	0.9
	5.0	20.7	18.0	0.9
	10.0	12.9	14.8	6.1
$SrIrO_3$/$SrTiO_3$ ($\varepsilon = -1.4\%$)	2.0	41.6	35.9	1.0
	5.0	25.3	57.8	1.3
	10.0	19.3	28.8	1.3
$SrIrO_3$/LSAT ($\varepsilon \approx -2.3\%$)	2.0	9.1	19.1	6.3
	10.0	9.6	13.3	1.7
$SrIrO_3$/$NdGaO_3$ ($\varepsilon \approx -2.5\%$)	2.0	16.2	36.7	12.4
	10.0	10.0	15.1	1.8

Table 1. Characteristic lengths obtained from the Maekawa–Fukuyama fit for films deposited on four different substrates.

Acknowledgements

The authors thank V. A. Baydikova, N. V. Dubitskiy, Yu. V. Kislinskii, A. V. Shadrin for sample fabrication and help with the X-ray analysis, and D. B. Migas and A. L. Danilyuk for useful discussions. This work was supported by the Russian Science Foundation, grant No. 23-79-00010.

Contact information

Corresponding author: G. D. Ulev,
orcid.org/0009-0009-9070-1524,
e-mail ulev.gd@phystech.edu

* This paper is based on a talk presented at the II International Scientific Conference "Advanced functional materials for digital and quantum electronics 2026", September 14–18, 2026, Dolgoprudny, Russia.

References

[1] Carter J. M., Shankar V. V., Zeb M. A., Kee H.-Y. *Semimetal and topological insulator in perovskite iridates.* Phys. Rev. B, vol. 85, 115105 (2012).

[2] Liu Z. T., Li M. Y., Li Q. F., Liu J. S., Li W., Yang H. F., Yao Q., Fan C. C., Wan X. G., Wang Z., Shen D. W. *Direct observation of the Dirac nodes lifting in semimetallic perovskite $SrIrO_3$ thin films.* Sci. Rep., vol. 6, 30309 (2016).

[3] Groenendijk D. J., Autieri C., Girovsky J., Martinez-Velarte M. C., Manca N., Mattoni G., Monteiro A. M. R. V. L., Gauquelin N., Verbeeck J., Otte A. F., Gabay M., Picozzi S., Caviglia A. D. *Spin-Orbit Semimetal in the Two-Dimensional Limit.* Phys. Rev. Lett., vol. 119, 256403 (2017).

[4] Danilyuk A. L., Podryabinkin D. A., Filonov A. B., Ovsyannikov G. A., Ulev G. D., Constantinian K. Y., Migas D. B. *Low temperature 2D quantum corrections to magnetoconductance in thin iridate films.* Solid State Commun., vol. 406, 116220 (2025).

[5] Baydikova V. A., Dubitskiy N. V., Petrzhik A. M., Ovsyannikov G. A., Moskal I. E., Shadrin A. V., Nagornykh K. E. *Effect of Epitaxial Stresses on the Structure and Electron Transport in Strontium Iridate Thin Films.* Phys. Met. Metallogr., vol. 126, 1652 (2025).

[6] Zhang L., Liang Q.-F., Xiong Y., Zhang B., Gao L., Li H., Chen Y. B., Zhou J., Zhang S., Gu Z., Yao S., Wang Z., Lin Y., Chen Y. F. *Tunable semimetallic state in compressive-strained $SrIrO_3$ films revealed by transport behavior.* Phys. Rev. B, vol. 91, 035110 (2015).

[7] Maekawa S., Fukuyama H. *Magnetoresistance in Two-Dimensional Disordered Systems: Effects of Zeeman Splitting and Spin-Orbit Scattering.* J. Phys. Soc. Japan., vol. 50, 2516 (1981).

[8] Altshuler B. L., Aronov A. G., Khmelnitsky D. E. *Effects of Electron-Electron Collisions with Small Energy Transfers on Quantum Localization.* J. Phys. C, vol. 15, 7367 (1982).

[9] Nagaosa N., Sinova J., Onoda S., MacDonald A. H., Ong N. P. *Anomalous Hall effect.* Rev. Mod. Phys., vol. 82, 1539 (2010).

[10] Ulev G. D., Ovsyannikov G. A., Constantinian K. Y., Moskal I. E. *Anomalous Hall effect in epitaxial strained iridate thin films.* JETP Lett., vol. 124, 225 (2026).